

# MAGNETIC FIELDS OF COALESCING NEUTRON STARS AND THE LUMINOSITY FUNCTION OF SHORT GAMMA-RAY BURSTS

K. A. Postnov, A. G. Kuranov

*Sternberg Astronomical Institute, 119992, Moscow, Russia*

## Abstract

Coalescing neutron star binaries are believed to be the most reliable sources for ground-based detectors of gravitational waves and likely progenitors of short gamma-ray bursts. In the process of coalescence, magnetic fields of neutron stars can induce interesting observational manifestations and affect the form of gravitational wave signal. In this paper we use the population synthesis method to model the expected distribution of neutron star magnetic fields during the coalescence under different assumptions on the initial parameters of neutron stars and their magnetic field evolution. We discuss possible electromagnetic phenomena preceding the coalescence of magnetized neutron star binaries and the effect of magnetic field on the gravitational wave signal. We find that a log-normal (Gaussian in logarithms) distribution of the initial magnetic fields of neutron stars, which agrees with observed properties of radio pulsars, produces the distribution of the magnetic field energy during the coalescence that adequately describes the observed luminosity function of short gamma-ray bursts under different assumptions on the field evolution and initial parameters of neutron stars. This agreement lends further support to the model of coalescing neutron star binaries as progenitors of gamma-ray bursts.

## 1 Introduction

Neutron stars (NS) are end products of thermonuclear evolution of stellar cores with a mass above  $\sim 8 - 10M_{\odot}$ . The birth of a NS in the core collapse is accompanied by the ejection of the outer stellar envelope which is observed as type II or Ib/c supernova, depending on the evolutionary status of the star immediately before the collapse. Young NS observed as radio pulsars demonstrate large space velocities (typically several hundreds km/s, see e.g. Hobbs et al. 2005), which is commonly explained by a hypothetical kick

velocity acquired by a nascent NS during the collapse. Different physical mechanisms of the kicks are discussed in the literature (e.g. Lai 2001).

It is well known that astrophysical manifestations of a NS at all evolutionary stages are determined by its spin, magnetic field, and the interaction with the of the surrounding medium (see Lipunov 1992). The evolution of a NS in a binary system is even more complicated by the presence of the secondary component. So the properties of the galactic population of NS in binaries are subjected to uncertainties in the theory of evolution of binary stars, such as the initial orbital parameters of binary stars, uncertainties in the description of the evolutionary mass loss of normal stars via stellar winds, the efficiency of common envelopes, etc. Binary NS observed as a specific subclass of binary pulsars are of special interest. Close binary NS (also called relativistic double stars) are considered as best sources of gravitational waves to be observed by the present-day gravitational wave detectors (Grishchuk et al. 2001). The evolution of relativistic binaries and binary pulsars is considered in more detail in many reviews (see, e.g., Postnov and Yungelson (2006), Bisnovaty-Kogan (2006)). The coalescence of binary NS due to secular decrease of the orbit because of orbital angular momentum removal by gravitational waves can be the primary formation channel of short hard gamma-ray bursts (Blinnikov et al. 1984, Eichler et al. 1989, see Nakar 2007 for extensive review).

Magnetic fields of coalescing NS binaries can lead to interesting observational manifestations preceding the gravitational wave burst (e.g. Lipunov and Panchenko 1996, Lipunova et al 1997), and can play a significant role in shaping the expected form of gravitational wave signal (Lipunova and Lipunov 1998). The recent general relativistic numerical calculations of coalescence of magnetized double NS (Yuk Tun Li et al. 2008) confirmed the crucial role of strong magnetic field in delaying the collapse of an intermediate super-massive object that forms during the coalescence process. Obviously, the magnetic field cannot be neglected when calculating the gravitational-wave templates from coalescing NS binaries, which is very important for ongoing gravitational wave detectors (Braginsky 2008, Abbott et al. 2008).

The population synthesis method is a powerful tool to study astrophysical manifestations of NSs. It enables calculation of large ensembles of objects and testing different scenarios of their evolution (see, e.g., Popov and Prokhorov

2007 for more detail). This method, with different degree of account for features of binary star evolution, has been successfully applied to study the evolution of coalescing NS binaries by different authors (Tutukov and Yungelson 1994, Lipunov et al. 1997, Portegies Zwart and Yungelson 1998, Belczynski et al. 2008). In recent papers (Postnov and Kuranov 2008, Kuranov et al. 2009), the population synthesis method was applied to study the effect of the possible kick-spin correlation on the coalescence rate of binary NSs and the observed correlation of the spin axis of radio pulsars with the direction of their space velocities.

In the present work we use the Scenario Mashine code (see the detailed description in Lipunov et al. 2009) to calculate the expected distribution of magnetic fields in coalescing binary NSs under different assumptions on the initial distribution of NS magnetic field and its evolution (no field decay or accretion-induced decay). The calculated distribution of magnetic fields is compared with the observed luminosity function of short gamma-ray bursts. It is shown that for the initial log-normal distribution of NS magnetic fields, which well describes observational properties of radio pulsars, the calculated distribution of the magnetic energy (both the energy of the poloidal magnetic field and the total magnetic field including the toroidal component) in coalescing binaries well fits the observed luminosity function of short gamma-ray bursts if one assumes that the total energy release in a gamma-ray burst formed during the coalescence is proportional to the total magnetic field energy. The agreement is achieved in different models of the NS magnetic field evolution (the field decay time, accretion-induced decay) and initial parameters of young NS (the amplitude of natal kick velocity and its possible correlation with the NS spin).

## 2 THE MODEL

### 2.1 *Magnetic fields of neutron stars*

The initial magnetic field of neutron stars is one of the main parameters of our calculations. We used two possible forms of the initial magnetic field distribution of NSs: 1) log-normal distribution of dipole magnetic moments

$\mu$ :

$$f(\mu) d\mu \propto \exp \left[ -\frac{(\log \mu - \log \mu_0)^2}{\sigma_\mu^2} \right] d\mu, \quad (1)$$

and 2) plain in logarithm distribution:

$$f(\mu) d\mu \propto \frac{\log \mu}{\log \mu_{\max} - \log \mu_{\min}} d\mu. \quad (2)$$

The first law directly follows from the analysis of the observed properties of radio pulsars and the field estimation using pulsar spin period and its first derivative (see the ATNF pulsar catalogue, Hobbs and Manchester 2009). The second law covers a broad range of magnetic field values and assumes an equal birth probability for strong-field NSs (like magnetars) and low-field NSs (like anti-magnetars, i.e. radio pulsars with low surface fields and slow rotation). Indeed, some recent studies (e.g. Woods 2008) suggest the birthrate of magnetars comparable with that of ordinary pulsars, and one of the youngest NSs in the center of the supernova remnant Cas A is likely to be an anti-magnetar (Gotthelf and Halpern 2008). Of course, the NS magnetic field at birth can depend on the NS parameters (for example, on its angular momentum), but in view of the existing uncertainty in NS formation theory we do not consider such a complication of the initial conditions.

In our calculations we adopted the following parameters of the initial distribution of the NS dipole magnetic moment (Faucher-Giguere and Kaspi 2006):

$$\begin{aligned} \log \mu_0 &= 30.35 \quad , \quad \sigma_\mu = 0.55, \\ \mu_{\min} &= 10^{26} \text{ }^3 \quad (B_{\min} = 10^8 \text{ }^3), \\ \mu_{\max} &= 10^{32} \text{ }^3 \quad (B_{\max} = 10^{14} \text{ }^3), \end{aligned} \quad (3)$$

(the NS surface magnetic field  $B$  is calculated for the assumed NS radius  $R_{\text{NS}} = 10 \text{ km}$ ).

## 2.2 Magnetic field evolution

The evolution of the NS magnetic field is poorly known. It follows from general theoretical considerations that poloidal magnetic fields of single NSs

must decay due to Ohmic losses in the crust (Flowers and Ruderman, 1977) with the characteristic time longer than  $\sim 10^7$  yrs. Observational tests of this hypothesis yield controversial results. For example, the analysis of statistical properties of radio pulsars leads some authors to conclude that the magnetic field of NSs must decay with the characteristic time  $\sim 3$  mln yrs (Gontier et al 2004), while another authors argue that statistical properties of radio pulsars do not require any magnetic field decay on timescales as long as comparable to the pulsar life time  $\sim 100$  mln yrs (Faucher-Giguere and Kaspi 2006).

In our calculations we used the following parametrization of the NS magnetic field evolution with time:

$$\mu = \begin{cases} \mu_0 e^{-t/\tau}, & \mu > \mu_{\min}, \\ \mu_{\min}, & t > \tau \ln(\mu_0/\mu_{\min}). \end{cases} \quad (4)$$

The characterisitic decay time of the dipole magnetic field was chosen from  $\tau = 10^7$  yrs to  $\infty$  (no decaY), and the minimum possible NS magnetic dipole moment was taken to be  $\mu_{\min} = 10^{26}$  G $\cdot$ cm<sup>3</sup>, which corresponds to a NS surface field of  $B \simeq 10^8$  G.

Indeed, observations and theoretical arguments suggest that the surface poloidal magnetic field of an accreting NS in a close binary system must asymptotically decay (Bisnovaty-Kogan and Komberg 1974, Taam and Van den Heuvel 1986, Romani 1990, Bhattacharia 2002) down to a lower limit of  $10^8 - 10^9$  G (Kulkarni 1986, Van den Heuvel et al. 1986). The magnetic field decay in accreting NSs was accounted for in the form (Romani 1990):

$$\mu = \mu_0(1 + 10^6 \Delta m)^{-0.8}, \quad (5)$$

where  $\mu_0$  and  $\mu$  are the value of the NS dipole magnetic moment before and after the accretion stage, respectively,  $\Delta m$  is the mass of accreted matter (in solar masses).

### 2.3 Toroidal field of NSs

The stability analysis of an axisymmetric magnetic field (Prenderghast 1956, Tayler 1973, Wright 1973) suggests that a substantial fraction of the total

magnetic field energy of a NS is contained in the toroidal component. Each field component (poloidal or toroidal) are separately unstable but can be stabilized by the presence of another component. The stability criterion of an axisymmetric magnetic field depends on several parameters and for a NS can be expressed in terms of the ratio of the energy of the poloidal component  $E_p$  to the total magnetic energy of the star  $E_m = E_p + E_t$  (see Braithwaite 2008): the upper limit for stability is  $(E_p/E_m) \sim 0.8$ ; the lower limit for stability is  $(E_p/E_m)_{crit} \sim 10^3 E_m / |E_{gr}|$ . Here  $E_{gr}$  is the gravitational binding energy ( $\sim 10^{53}$  erg). In our calculations we assumed that the NS magnetic field always satisfies this stability criterion, i.e. for a given value of  $E_p(t)$  the total magnetic field energy  $E_m(t)$  falls within the stability limits

$$1.25E_p(t) < E_m(t) < 10^{-3} \sqrt{E_p(t)|E_{gr}|}. \quad (6)$$

#### 2.4 Kick velocity during NS or BH formation

The collapse asymmetry leads to additional kick velocity to a newborn NS. We modeled this velocity as follows: the direction of the kick velocity vector was taken to lie randomly within a cone with angle  $\theta$  around the rotational axis of the pre-supernova, and its absolute value was assumed to be distributed according to a Maxwellian law:

$$f(v) dv \propto \exp\left(-\frac{v^2}{V_m^2}\right) v^2 dv, \quad (7)$$

where  $V_m$  is the characteristic velocity.

We have used two frequently considered kick velocity distributions (see the discussion in review Postnov and Yungelson (2006) and in the recent paper Martin et al. 2009).

**Model .** Single-mode Maxwellian distribution. All NSs acquire kick velocity at birth. The parameter  $V_m$  varies within the range 100 – 500 km/s.

**Model .** Bimodal Maxwellian distribution. For the components of close binary system (here we call a system as close binary if one of the components

filled its Roche lobe and mass transfer occurred at some stages preceding the core collapse supernova of the primary component) with initial masses  $8M_{\odot}$ – $11M_{\odot}$ , the electron-capture supernova from degenerate O-Ne-Mg stellar core is assumed. In that case the natal kick is small or zero. This assumptions allows one to explain some observational properties of X-ray Be-systems and binary pulsars (see Podsiadlowski et al 2004, Van den Heuvel 2004, 2007). In Model B with bimodal kick we assumed  $V_m = 30$  / for a pre-supernova with the initial mass from the range  $8M_{\odot}$ – $11M_{\odot}$  and the mass transfer stage took place before the collapse. In other cases (i.e. for NS born from single progenitors or binary components with the initial mass above 11 solar masses) the parameter  $V_m$  varied within the range  $100 - 500$  km/s, as in Model A. So

$$V_m = \begin{cases} 100...500\text{km/s,} & > 10M_{\odot}, & \text{Model A} \\ 100...500\text{km/s,} & > 11M_{\odot}, & \text{Model B} \\ 30\text{km/s,} & 8M_{\odot}-11M_{\odot}, \text{closebinary} & \end{cases}$$

For both kick models we assumed all single NSs and NSs in wide binaries to have the initial mass  $M_{\text{NS}} = 1.4M_{\odot}$ . In model B, NSs formed from e-capture SN are assumed to have smaller initial masses  $M_{\text{NS}} = 1.25M_{\odot}$ .

### 3 RESULTS OF POPULATION SYNTHESIS CALCULATIONS

The models of the natal kick and magnetic field evolution of netron stars are listed in Table 1. The results of calculations of different models are presented in Fig. 1-5. For each model, calculations were performed for isotropic kicks (corresponding to  $\theta = 90^\circ$ ) and kicks collimated with the rotational axis of the NS within the cone  $\theta = 10^\circ$ . This value of  $\theta$  is suggested by the recent analysis of the spin-velocity alignment of radio pulsars (Kuranov et al. 2009).

Fig. 1 shows the integral distribution of the binary NS coalescence rate as a function of the time of coalescence (determined as the time interval from the formation of a double NS binary until its merging due to gravitational wave emission) for different models of NS formation (models A and B). The total (over galactic lifetime) binary coalescence rate is a few times higher in Model B than in Model A (see also Postnov and Kuranov 2008), which is naturally

related to decrease in the binary disruption probability during formation of low-kick NSs in Model B. A strong dependence of the NS binary coalescence rate on the kick-spin alignment effect characterized by the value of the angle  $\theta$  can also be seen. For small  $\theta$  (strong alignment) the mean time of NS binary coalescence increases, so mainly old NSs coalesce. With increasing angle  $\theta$  (the kick isotropisation) the fraction of young coalescing NSs with high magnetic field increases, since for isotropic kicks there is a certain probability for the NS to get kick directed oppositely to the orbital motion at the moment of explosion. Correspondingly, the fraction of coalescing highly magnetized NSs is maximum for isotropic kicks when  $\theta = 90^\circ$ , see Fig. 2.

Fig. 2 shows the distribution of NS dipole momenta (in units  $\mu_{30} = \mu/(10^{30} \text{ G cm}^3)$ ) at the coalescence for the tight kick-spin alignment (upper panel) and the isotropic kick (bottom panel) for a log-normal initial magnetic field distribution (Model BG8). In Fig. 3 an integral distribution of the minimum (left plots) and maximum (right plots) magnetic moments of the components of coalescing double NSs are presented for different models. Plots in upper and bottom panels are calculated for the initial log-normal (Model BG8) and log-flat (Model BF8) field distributions, respectively. The two-dimensional distribution of magnetic moments of both components at coalescence is plotted in Fig. 4 for the log-normal initial distribution (model BF8). The minimum  $E_m^{min}$  and maximum  $E_m^{max}$  values of the total magnetic field energy of the coalescing binary components (satisfied to the stability criterion (6)) in Model BG8 is shown in Fig. 5.

## 4 DISCUSSION

The calculated magnetic field distribution of coalescing NSs has several astrophysical implications.

### 1) Electromagnetic precursors of short gamma-ray bursts.

A coalescing NS binary that leads to a powerful gamma-ray burst (Blinnikov et al. 1984, Eichler et al. 1989, see Nakar 2007 for a review) can be preceded by an electromagnetic burst (Lipunov and Panchenko 1996). Assuming the Goldreich-Julian current in the relativistic wind along open magnetic field



lines and the light cylinder radius  $R_l = c/\Omega \gg a$ , which are determined by the rotation of the magnetized NS, we obtain the standard estimation of the total EM losses (e.g. Beskin 2009)

$$W_{em} \sim (\Omega R/c)^4 B^2 R^2 c \sim \Omega^4 \mu^2 / c^3 \quad (8)$$

(here  $\Omega = 2\pi/P$  is the spin frequency of the NS,  $R$  is its radius,  $\mu = BR^3$  is the NS dipole magnetic moment,  $a$  is the radius of the circular orbit,  $c$  is the speed of light). Assuming that the NS rotation is synchronized with its orbital revolution at final stages before the coalescence, i.e.  $\Omega^2 = 2GM/a^3$  (the 3-d Kepler law for two equal-mass NS in the circular orbit with semi-major axis  $a$ ), we obtain

$$W_{em} \sim 3 \times 10^{39} (\text{erg/s}) \mu_{30}^2 (M/M_\odot)^2 (a/10^7 \text{cm})^{-6}.$$

The characteristic values of the magnetic field of the second (younger) NS in the binary in the considered models is  $\mu_{30}(NSII) \sim 10 - 10^{-4}$  (see Fig. 3), and we obtain a total EM power emitted before the coalescence within the range from  $\sim 10^{32}$  to  $\sim 10^{42}$  erg/s, with the energy release strongly increasing with orbital decrease as  $1/a^6$ .

In the relativistic particle wind flowing along open field lines plasma instability can develop to generate high-frequency radio emission, as in radio pulsars. The efficiency of conversion of the total power released into radio emission is fairly small in radio pulsars,  $\sim 10^{-5} - 10^{-6}$ , so even during last orbital revolutions before the coalescence the expected power of a radio burst is hardly to be more than  $\sim 10^{42}$  erg/s. In principle, this power is sufficient to explain properties of the unique extragalactic 5-ms radio burst (Lorimer et al 2007). However, such a powerful radio burst would require a significant dipole magnetic field of the NS at coalescence,  $\mu_{30} \gg 1$ . Fig. 3 shows that for the most favorable models with narrow kick-spin alignment the fraction of such highly magnetized NS is of order of a few per cents of the total number of coalescing NS binaries. This aggravates the low-event-rate problem for the explanation of the observed ms radio burst by the binary NS coalescence model (Lorimer et al 2007, Popov and Postnov 2007). On the other hand, in this model there is no problem for the highly coherent radio emission to go out of the generation region due to induced scattering (Lyubarsky 2008), which must be overcome in other models for this radio burst (e.g. Egorov and Postnov 2009). The fact that the observed ms radio burst was not associated with a gamma-ray burst could be due to different beaming angles for

the pre-outburst radio emission and the subsequent gamma-ray burst. Low statistics (one event), however, makes the statistical arguments very weak, so the possibility to explain this radio burst by mechanism proposed by Lipunov and Panchenko (1996) still remains.

## 2) The effect of the magnetic field of coalescing NSs on the form of the gravitational wave signal

Yuk Tun Li et al (2008) studied numerically the effect of a strong magnetic field of the components of a coalescing NS binary on the form of the emitted gravitational wave (GW) signal at the stage preceding the merging of the components. In their numerical relativistic calculations, these authors used models of non-rotating NSs with a strong ( $B \sim 10^{16}$  G) poloidal magnetic field. The difference in the GW signal form turned out to be significant if the final collapse of the supramassive differentially rotating NS (formed in the merging) into a black hole is magnetically delayed. Our calculations show that even for the initial high (magnetar-like) magnetic fields, the vast majority of coalescing NSs has significantly (by orders of magnitude) smaller magnetic fields if the field decay is assumed (Fig. 4). However, internal toroidal magnetic field can be much higher than the poloidal component, so that the energy of the magnetic field at coalescence can be mostly determined by the toroidal component and be as high as  $10^{47}$  ergs (and even more if one assumes the initial fields as high as  $\sim 10^{15} - 10^{16}$  G). Although such a field can not be too significant dynamically ( $E_m/|E_{gr}| \sim 10^{-5} - 10^{-6}$ ), it may serve as a seed field for the magnetic field generation in a merged differentially rotating object. In principle, following arguments by Spruit (2008), the energy of differential rotation of the pre-collapsed merged object may entirely be transformed into the magnetic field energy, so that

$$B^2 R^3 \sim (\Delta\Omega/\Omega)^2 E_{rot}, \quad (9)$$

where  $R$  is the radius of the object, the factor  $\Delta\Omega/\Omega$  takes into account the differential rotation and  $E_{rot}$  is the rotational energy. Assuming similar field generation processes to operate in a differentially rotating proto-NS and the pre-collapsing post-merging object, the magnetic field can be of order to  $B_{max,coal} \sim B_{max,NS}(E_{rot,coal}/E_{rot,NS})^{1/2}$ . Limiting  $E_{rot,NS}$  from above by the value  $\sim 10^{51}$  ergs (Spruit 2008) and assuming the virial value of  $E_{rot,coal}$  of order of the binding energy of the NS  $\sim 10^{53}$  ergs, we obtain the potentially possible energy of the poloidal magnetic field of pre-collapsing post-merging

object about  $\sim 10$  times higher than for a young NS. This energy can be dynamically significant for the subsequent evolution of this object and must be taken into account in calculations of the expected form of the GW signal at post-merging phases.

### 3) The luminosity function of short gamma-ray bursts

Probably, the most intriguing implication of our calculations relates to short gamma-ray bursts. Presently, the merging of compact NS binaries is thought to be the principal formation channel of short hard gamma-ray bursts (Blinnikov et al. 1984, Eichler et al. 1989, see Nakar 2007 for a recent review). The plausible physical mechanism of generation of hard electromagnetic gamma-radiation during the NS binary coalescence is related to the formation of ultra-relativistic MHD jet (Usov 1992, see recent numerical calculations by Komissarov et al. 2009). The NS magnetic field can be an important initial parameter for such a jet formation. Indeed, the power of energy release in the MHD-mechanism is roughly  $L \sim B^2 \omega^4 R^6$ , where  $\omega$  is the characteristic spin frequency,  $R$  is the radius and  $B$  is the magnetic field strength. For different coalescing NS binaries parameters  $\omega$  and  $R$  are most likely similar, while the value of the magnetic field strength can be significantly different. Of course, as we argued above, the magnetic field can strongly increase during the coalescence process, however immediately before the merging NS fields serve as the initial conditions. Thus, *there are physical grounds to expect that the distribution of luminosities of short gamma-ray bursts  $\Phi(L)$  will reflect the distribution of magnetic fields of coalescing NSs:  $d\Phi(L)/dL \propto dN/dB$ .*

We shall consider two different possibilities.

- 1)  $\Phi(L)$  reflects distribution of the energy of the NS poloidal field  $E_p$   $B_p^2$  before the coalescence,

$$\Phi(L) \propto dN/dE_p \propto dN/d(B_p^2).$$

and

- 2)  $\Phi(L)$  reflects the distribution of the total magnetic field energy (including the toroidal component)  $E_m = E_p + E_t$ . According to the stability criterion for the poloidal magnetic field (6), the maximum total energy of the magnetic field scales as  $E_m \sim \sqrt{|E_{gr}|E_p} \propto B_p$ , i.e. for a given value of the poloidal field

strength  $B_p$ , the distribution of the maximum possible magnetic field energy in a stable configuration is proportional to that of the poloidal magnetic field strength,

$$\Phi(L) \propto dN/dE_m \propto dN/dB_p.$$

Our calculations of magnetic fields of coalescing NS binaries allows testing these hypotheses. To this aim, we shall use the luminosity function of short gamma-ray bursts calculated using observational data for short gamma-ray bursts obtained by space observatories *Swift*, *INTEGRAL*, *Fermi* (Kann et al 2008). In Figs. 6 - 7 the integral luminosity function of short gamma-ray bursts  $N(> L)$  is shown by the solid black line connecting solid diamonds. The dashed lines show  $1-\sigma$  errors of the total GRB luminosity estimation  $L_\gamma$  (assuming spherical symmetry of emission) taken from Table 1 of Kann et al. (2008). In Fig. 6 we compare the hypothesis  $L_\gamma \propto B_p^2$  for different initial NS parameters (the natal kick velocity parameter  $V_m$ , spin-kick alignment angle  $\theta$ ) in our Models AG and BG (in which the NS magnetic field can decay only during accretion) with log-normal initial distribution of the poloidal magnetic field. The upper and lower panel of Fig. 6 show the comparison with the poloidal component of the second (younger) NS in the binary, the middle panel show the comparison with the field of the first (older) NS. It is seen that the observed short GRB luminosity distribution is in agreement with the distribution of magnetic fields of NS before the coalescence for any assumptions on the value and the direction of the natal NS kick velocity.

In Fig. 7 we compare the observed luminosity function of short gamma-ray bursts with the distribution of the total energy of the magnetic field before the coalescence (i.e. the hypothesis  $L_\gamma \propto E_m \propto B_p$ ) for models with exponential field decay AG8 (the upper panel) and BG8 (the bottom panel), as well as for a log-flat initial field distribution. For these models, the agreement with observations is reached for all values of narrow-collimated kicks ( $\theta = 10^\circ$ ), and cannot be reached at high values of the isotropic kicks ( $V_m = 500, 300$  km/s and  $\theta = 90^\circ$ ). The parameter of the Kolmogorov-Smirnov test for different models is listed in Table 2.

Note that in models with a logarithmically flat initial magnetic field distribution (our models AF, AF8, BF, BF8) the observed luminosity function of short gamma-ray bursts can not be described for any value and direction of

the NS kick.

## 5 CONCLUSIONS

Using the population synthesis method (the Scenario Mashine code), we have calculated the expected distribution of magnetic fields of coalescing binary neutron stars for various initial distributions and models of NS formation. We have taken into account both poloidal and toroidal components of the field satisfying the field stability criterion. The most important parameters of NS formation include the form (single-mode, bimodal Maxwellian distributions) and amplitude (30-500 km/s) of the natal kick velocity and its possible alignment with the NS spin. We have taken into account the NS magnetic field evolution (no decay, exponential decay until a bottom value of  $10^8$  G, accretion-induced decay). We discuss possible observational manifestations of the strong magnetic field of coalescing neutron stars (the electromagnetic precursors) and the effect of the magnetic field on the form of gravitational wave signal.

We have shown that the observed luminosity function of short/hard gamma-ray bursts is very well fitted by the magnetic field distribution of the coalescing neutron star binaries (the Kolmogorov-Smirnov test of order of one) for different initial NS formation models if the initial magnetic field distribution is taken in the log-normal form with parameters inferred from the radio pulsar observations. The obtained agreement of the distribution of magnetic fields of coalescing NS with the observed luminosity function of short gamma-ray bursts lends further support to the pioneer idea by Blinnikov et al. (1984) that coalescing NS binaries can be progenitors of cosmic gamma-ray bursts.

The work is supported by RFBR grant 07-02-00961.

1. Abbott B., Abbott R., Adhikari R. et al., 2008, Phys. Rev. D 77, Issue 6, 062002
2. Belczynski K., Kalogera V., Rasio F.A. et al., 2008, ApJS, 174, 223
3. Beskin V.S., 2009, MHD Flows in Compact Astrophysical Objects (Springer).
4. Bhattacharya D., 2002, J. Astrophys. Astron., 23, 67
5. Bisnovaty-Kogan G.S., 2006, Physics-Uspekhi, 49, 53
6. Bisnovaty-Kogan G.S., Komberg B.V., 1974, SvA 18, 217
7. Blinnikov S.I., Novikov I.D., Perevodchikova T.A., Polnarev A.G., 1984 SvAL, 10, 177
8. Braginsky V.B., 2008, Astron. Lett., 34, 558
9. Braithwaite J., 2008, MNRAS, 386, 1947
10. Egorov A.E., Postnov K.E., 2009, Astron. Lett., 35, 241
11. Eichler D., Livio M., Piran T., Schramm D.N., 1989, Nature, 340, 126
12. Faucher-Giguere C.A., Kaspi V.M., 2006, ApJ, 643, 332
13. Flowers E., Ruderman M.A., 1977, ApJ, 215, 302
14. Gonthier P.L., Van Guilder R., Harding A.K., 2004, ApJ, 604, 775
15. Gotthelf E.V., Halpern J.P., 2008, in 40 Years of pulsars. Ed. C.G. Bassa, Z. Wang, A. Cumming, V.M. Kaspi. Proc. AIP, v. 983, p. 320
16. Grishchuk L.P., Lipunov V.M., Postnov K.A., Prokhorov M.E., Sathyaprakash B., 2001, Physics-Uspekhi, 44, 1
17. Hobbs G.B., Lorimer D.R., Lyne A.G., Kramer N., 2005, MNRAS, 360, 974
18. Hobbs G.B., Manchester R.N, 2009, ATNF Pulsar Catalogue, v. 1.20, <http://www.atnf.csiro.au/research/pulsar/psrcat/>

19. Kann D.A., Klose S., Zhang B., Wilson A.C., Butler N.R., et al., 2008, arXiv:0804:1959
20. Komissarov S., Vlahakis N., Königl A., Barkov M.V., 2009, MNRAS, 394, 1182
21. Kulkarni S.R., 1986, ApJ, 306, L85
22. Kuranov A.G., Popov S.B., Postnov K.A., 2009, MNRAS, 395, 2087
23. Lai D., 2001, in Physics of Neutron Star Interiors, Edited by D. Blaschke, N.K. Glendenning and A. Sedrakian, Lecture Notes in Physics, vol. 578, p.424
24. Lipunov V.M., 1992, Astrophysics of Neutron Stars (Berlin: Springer)
25. Lipunov V.M., Panchenko I.E., 1996, Astron. Astrophys., 312, 937
26. Lipunov V.M., Postnov K.A., Prokhorov M.E., 1997, MNRAS, 288, 245
27. Lipunov V.M., Postnov K.A., Prokhorov M.E., Bogomazov A.I., 2009, Astron. Rep., in press [arXiv:0704.1387]
28. Lipunova G.V., Panchenko I.E., Lipunov V.M., 1997, New Astron., 2, 555
29. Lipunova G.V., Lipunov V.M., 1998, Astron. Astrophys., 329, 29
30. Lorimer D., Bailes M., McLaughlin M.A., Narkevic D.J., Crawford F., 2007, Science, 318, 377
31. Lyubarsky Yu., 2008, ApJ, 682, 1443
32. Martin R.G., Tout C.A., Pringle J.E., 2009, arXiv:0905.2362
33. Nakar E., 2007, Phys. Rep., 442, 166
34. Podsiadlowski P., Langer N., Poelarends A.J.T., et al., 2004, ApJ, 612, 1044
35. Popov S.B., Postnov K.A., 2007, arXiv:0710.2006
36. Popov S.B., Prokhorov M.E., 2007, Physics-Uspekhi, 50, 1123

37. Portegies Zwart S.F., Yungelson L.R., 1998, *Astron. Astrophys.*, 332, 173
38. Postnov K.A., Kuranov A.G., 2008, *MNRAS*, 384, 1393
39. Postnov K.A., Yungelson L.R., 2006, *Liv. Rev. Rel.* 9, 6
40. Prendergast K.H., 1956, *ApJ*, 123, 498P
41. Romani R., 1990, *Nature*, 347, 741
42. Spruit H.C., 2008, in *40 Years of Pulsars*. Eds. C.G. Bassa, Z. Wang, A. Cumming, V.M. Kaspi. *AIP Proc.* v. 983, p. 391
43. Taam R., van den Heuvel E.P.J., 1986, *ApJ*, 305, 235
44. Tayler R.J., 1973, *MNRAS*, 161, 365
45. Tutukov A.V., Yungelson L.R., 1994, *MNRAS*, 268, 871
46. Usov V.V., 1992, *Nature*, 357, 472
47. van den Heuvel E.P.J., van Paradijs J.A., Taam R.E.), 1986, *Nature*, 322, 153
48. van den Heuvel E. P. J., 2004, in *Proc. 5th Integral Science Workshop*, ed. V. Schönfelder, G. Lichti, & C. Winkler (ESA SP-552; Noordwijk), p. 185
49. van den Heuvel E.P.J., 2007, in *Proc. “The multicolored landscape of compact objects and their explosive origins”*, *AIP Conf. Proc.*, Vol. 924, p. 598 [arXiv:0704.1215]
50. Woods P.M., 2008, In *40 Years of pulsars*. Ed. C.G. Bassa, Z. Wang, A. Cumming, V.M. Kaspi. *Proc. AIP*, v. 983, p. 227
51. Wright G.A.E., 1973, *MNRAS*, 162, 339
52. Yuk Tung Li, Shapiro S.L., Etienne Z.B., Taniguchi K., 2008, *Phys. Rev. D* 78, 024012



Table 1. Models of the intital magnetic fields and natal kicks of NS

Model	Initial distribution of magnetic field	$B_p$ field decay time, yrs	$V_m$ Initial mass km s <sup>-1</sup>	of NS progenitor
<b>AG</b>	log-normal	$\infty$	100 ... 500	$> 10M_\odot$
			30	$8M_\odot-11M_\odot$
<b>BG</b>	log-normal	$\infty$	100...500	$> 11M_\odot$
<b>AG8</b>	log-normal	$10^8$	100 ... 500	$> 10M_\odot$
			30	$8M_\odot-11M_\odot$
<b>BG8</b>	log-normal	$10^8$	100...500	$> 11M_\odot$
<b>AF</b>	log-flat	$\infty$	100 ... 500	$> 10M_\odot$
			30	$8M_\odot-11M_\odot$
<b>BF</b>	log-flat	$\infty$	100...500	$> 11M_\odot$
<b>AF8</b>	log-flat	$10^8$	100 ... 500	$> 10M_\odot$
			30	$8M_\odot-11M_\odot$
<b>BF8</b>	log-flat	$10^8$	100...500	$> 11M_\odot$

Table 2. Kolmogorov-Smirnov test for the luminosity function of short gamma-ray bursts

Model	Tested hypothesis	$\theta$	$V_m=100 \text{ km s}^{-1}$	$V_m=300 \text{ km s}^{-1}$	$V_m=500 \text{ km s}^{-1}$
<b>AG</b>	$L_\gamma \propto E_p$	$10^\circ$	<b>0.904</b>	<b>0.995</b>	0.525
	$L_\gamma \propto E_p$	$90^\circ$	<b>0.991</b>	<b>0.999</b>	<b>1.000</b>
<b>BG</b>	$L_\gamma \propto E_p$	$10^\circ$	<b>0.999</b>	<b>0.997</b>	<b>1.000</b>
	$L_\gamma \propto E_p$	$90^\circ$	<b>0.893</b>	<b>0.947</b>	<b>1.000</b>
<b>AG8</b>	$L_\gamma \propto E_m$	$10^\circ$	<b>0.997</b>	<b>0.999</b>	<b>0.999</b>
	$L_\gamma \propto E_m$	$90^\circ$	0.469	2.6e-3	3.8e-4
<b>BG8</b>	$L_\gamma \propto E_m$	$10^\circ$	<b>1.000</b>	<b>1.000</b>	<b>1.000</b>
	$L_\gamma \propto E_m$	$90^\circ$	<b>0.999</b>	0.319	0.071

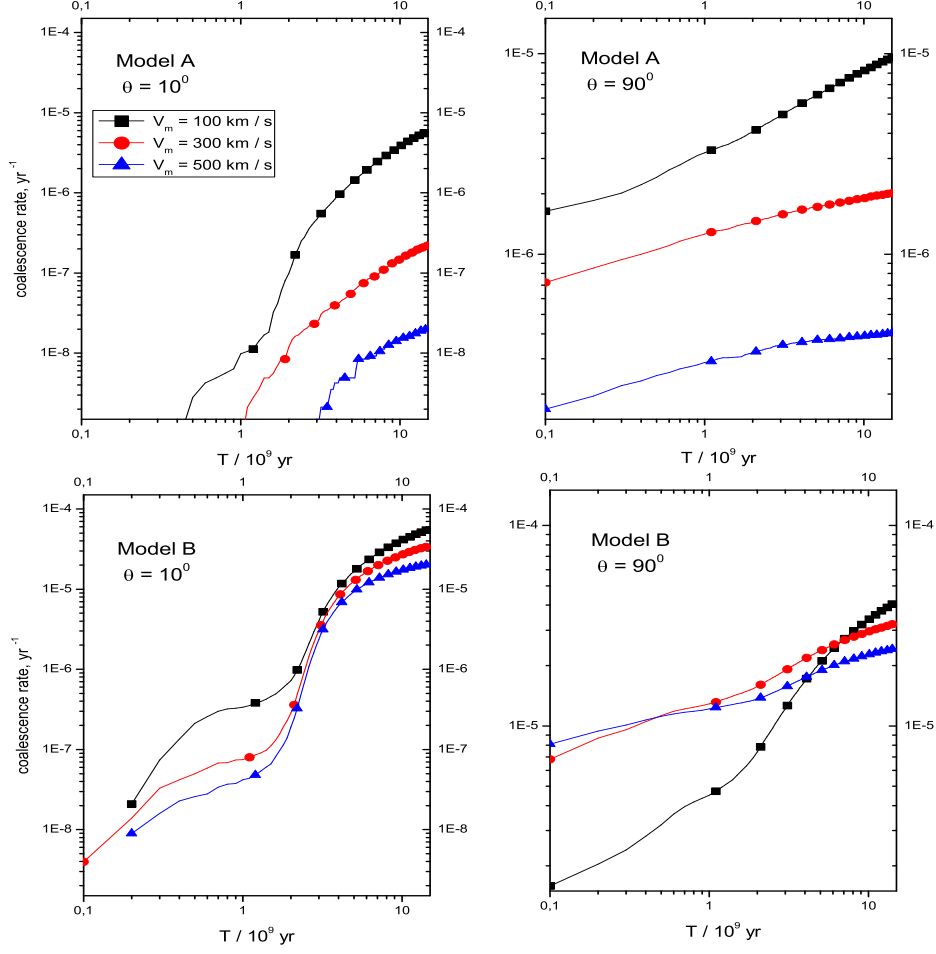


Figure 1. Integral distribution function of the binary NS coalescence rate as a function of time between the birth and merging for different NS formation parameters. The rate is normalized to the galactic star formation rate  $3M_{\odot}^{-1}$ . Upper plots: model A, bottom plots: model B. Plots to the left: the natal kick-spin alignment within the cone with angle  $\theta = 10^{\circ}$ . Plots to the right: the isotropical natal kick ( $\theta = 90^{\circ}$ ).

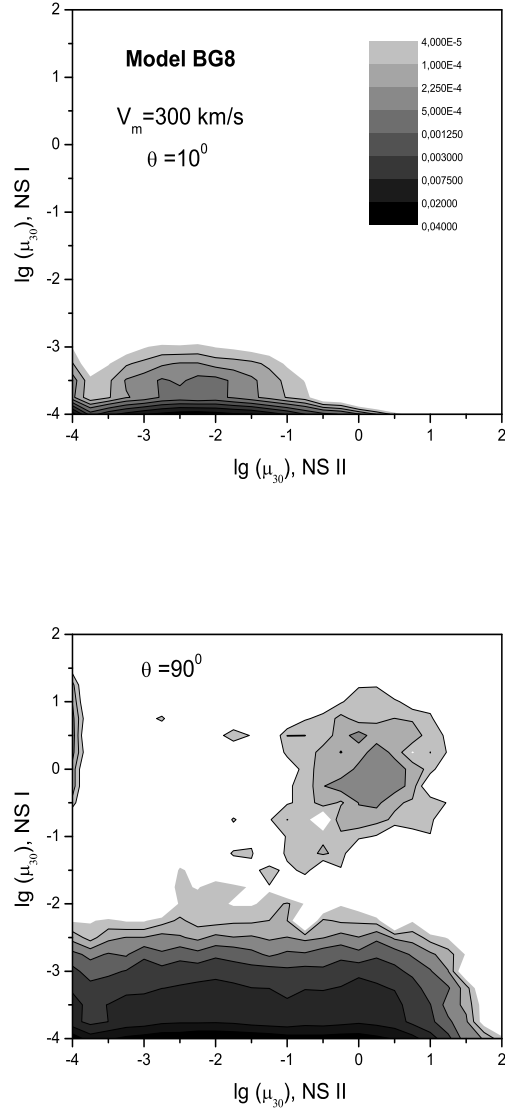


Figure 2. The distribution function of dipole magnetic moments of coalescing neutron stars (NS I denotes the first (older) NS, NS II – the second (younger) NS in the binary) by the moment of coalescence in Model BG8. The upper plot is calculated for narrow collimated kicks within  $\theta = 10^\circ$ . The bottom plots shows the result for isotropic kicks ( $\theta = 90^\circ$ ).

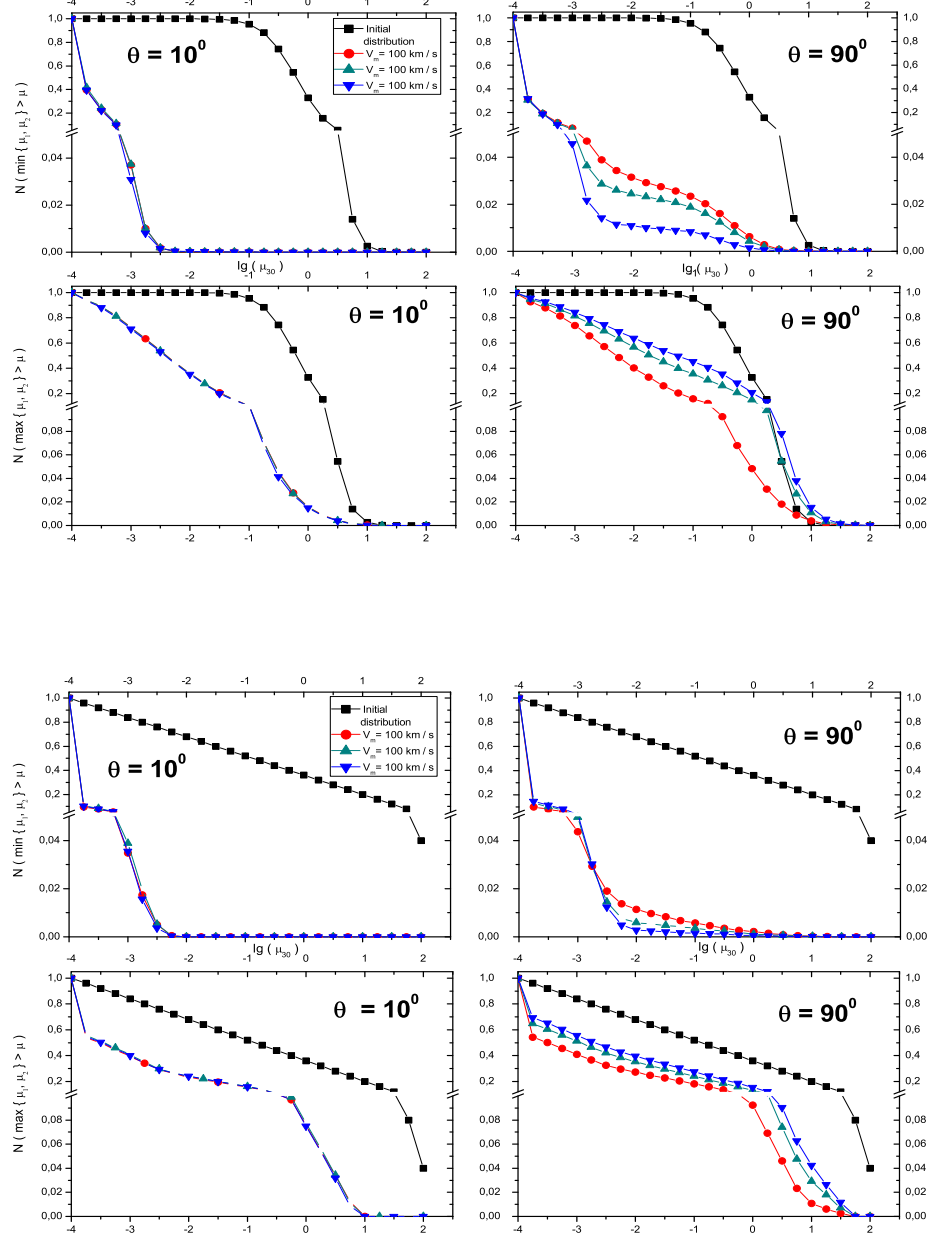


Figure 3. The integral distribution function of the minimum (to the left) and maximum (to the right) dipole moment of two binary NS components by the time of coalescence. The upper and bottom plots are calculated for Model BG8 and BF8, respectively. The angle  $\theta$  for natal kick-spin correlation is also shown.

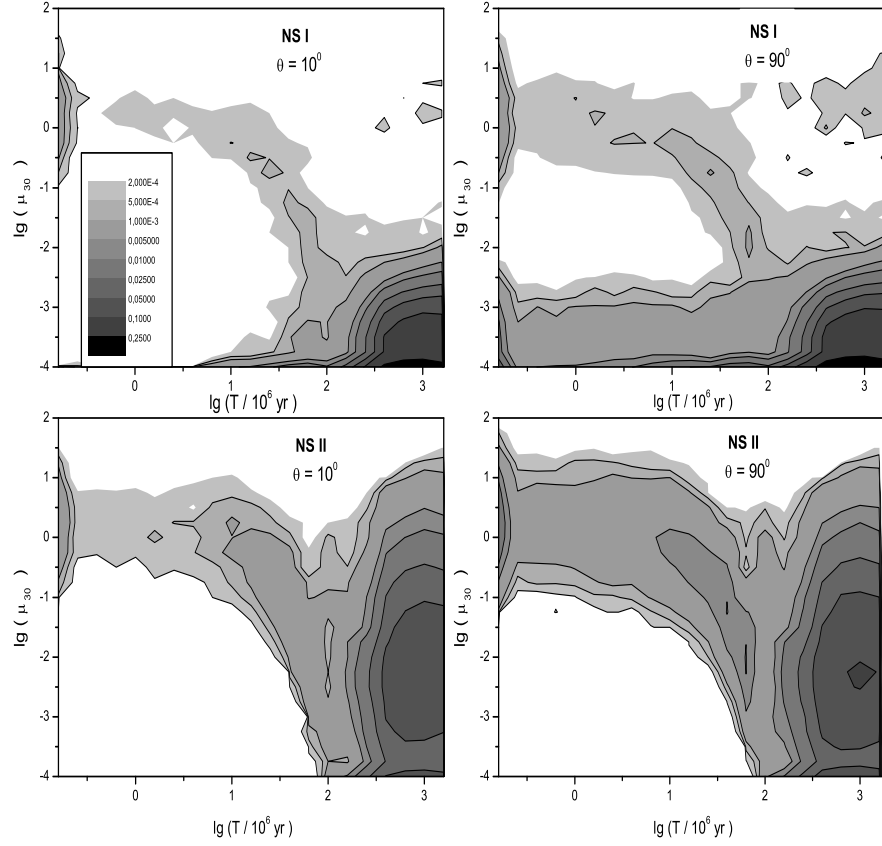


Figure 4. The distribution function of the dipole magnetic moments of the poloidal magnetic field and the coalescence time in Model BG8. The upper and bottom plot shows the distribution for the first (older) NSI and the second (younger) NSII, respectively. Left and right plots are for narrow-collimated ( $\theta = 10^\circ$ ) and isotropic ( $\theta = 90^\circ$ ) natal kicks, respectively.

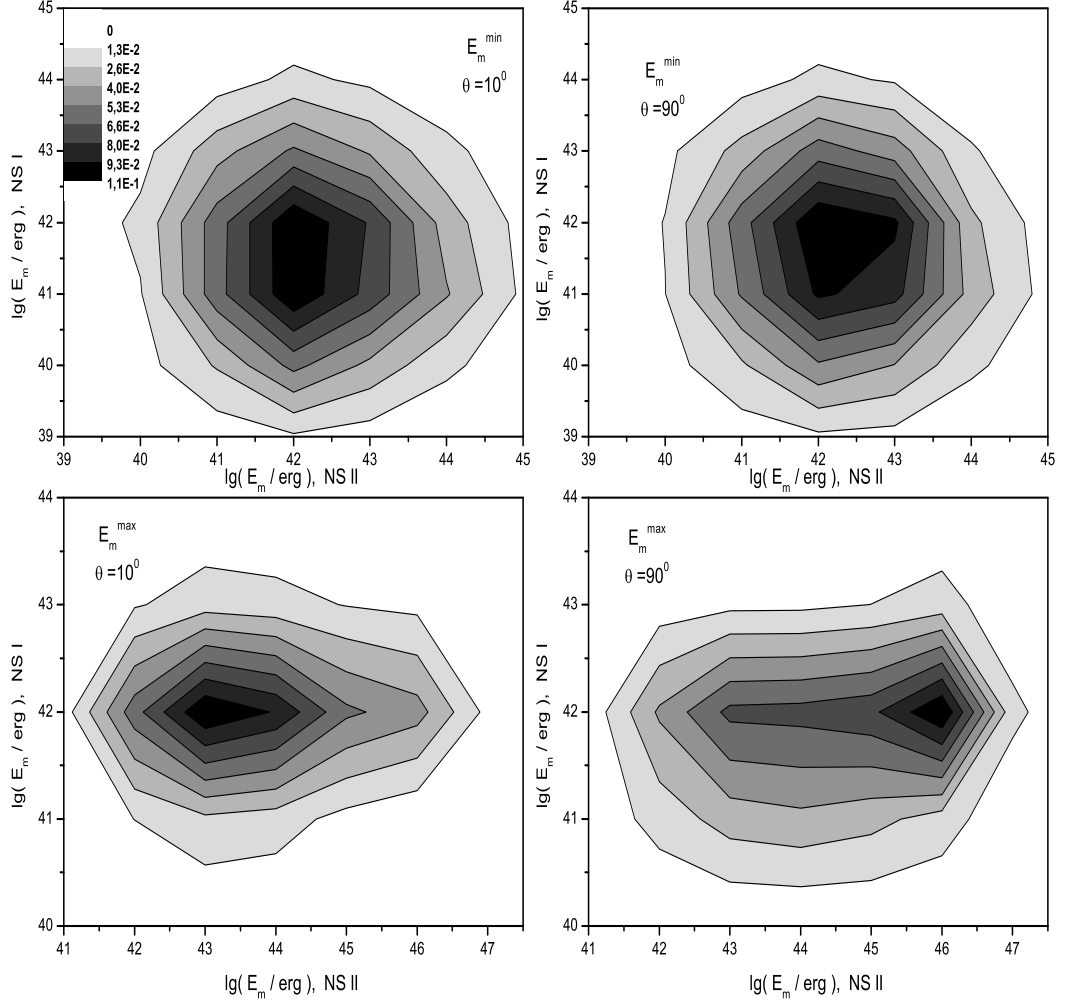


Figure 5. The minimum ( $E_m^{\min}$ , the upper panel) and maximum ( $E_m^{\max}$ , the bottom panel) total magnetic field energy of coalescing binary NS components by the time of coalescence. Model BG8.

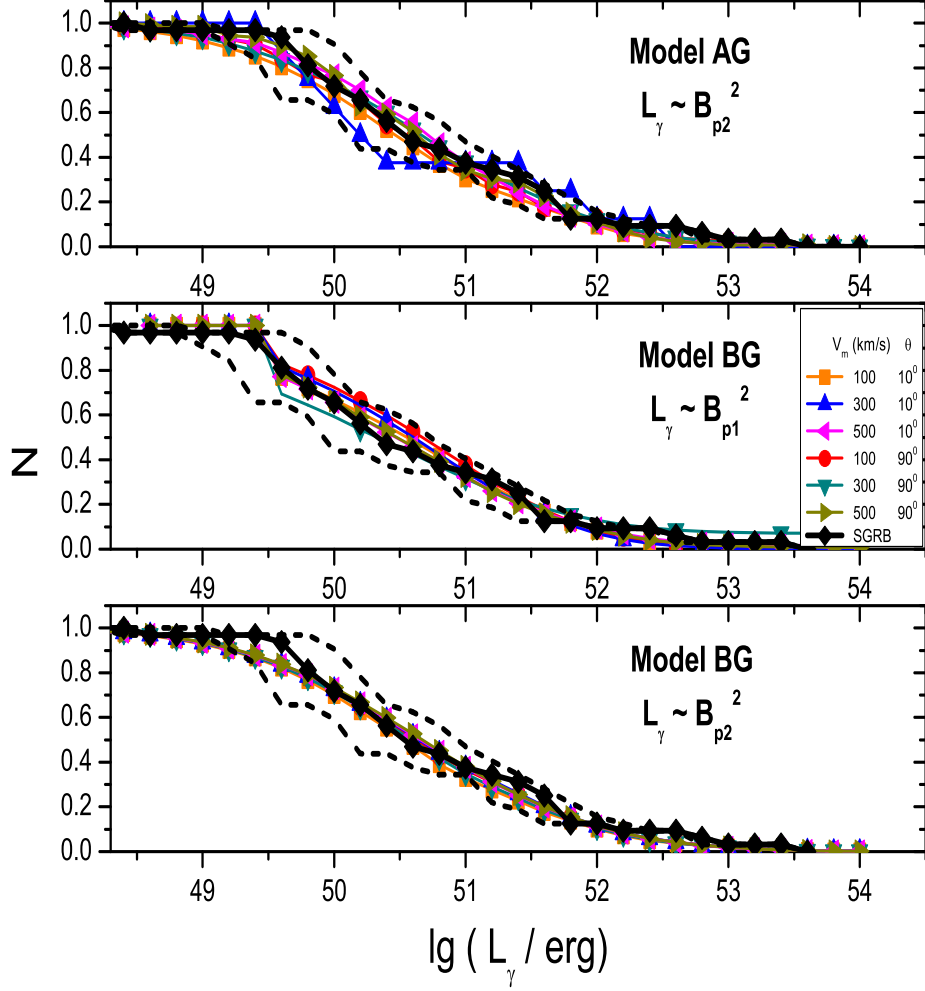


Figure 6. The comparison of the hypothesis  $L_\gamma \propto B_p^2$  for the luminosity of short gamma-ray bursts for different NS formation parameters in models AG and BG. On the top and bottom panel the comparison with the distribution of the poloidal field of the second (younger) NS in the binary is shown, while the plot on the middle panel is calculated for the field distribution of the first (older) NS. The observed integral distribution function of short gamma-ray bursts  $N(>L)$  as computed from data presented in Table 1 of Kann et al. (2008) is shown by the solid line connecting the filled diamonds. The dashed lines indicate  $1\text{-}\sigma$  errors of the gamma-ray burst luminosity  $L_\gamma$ .



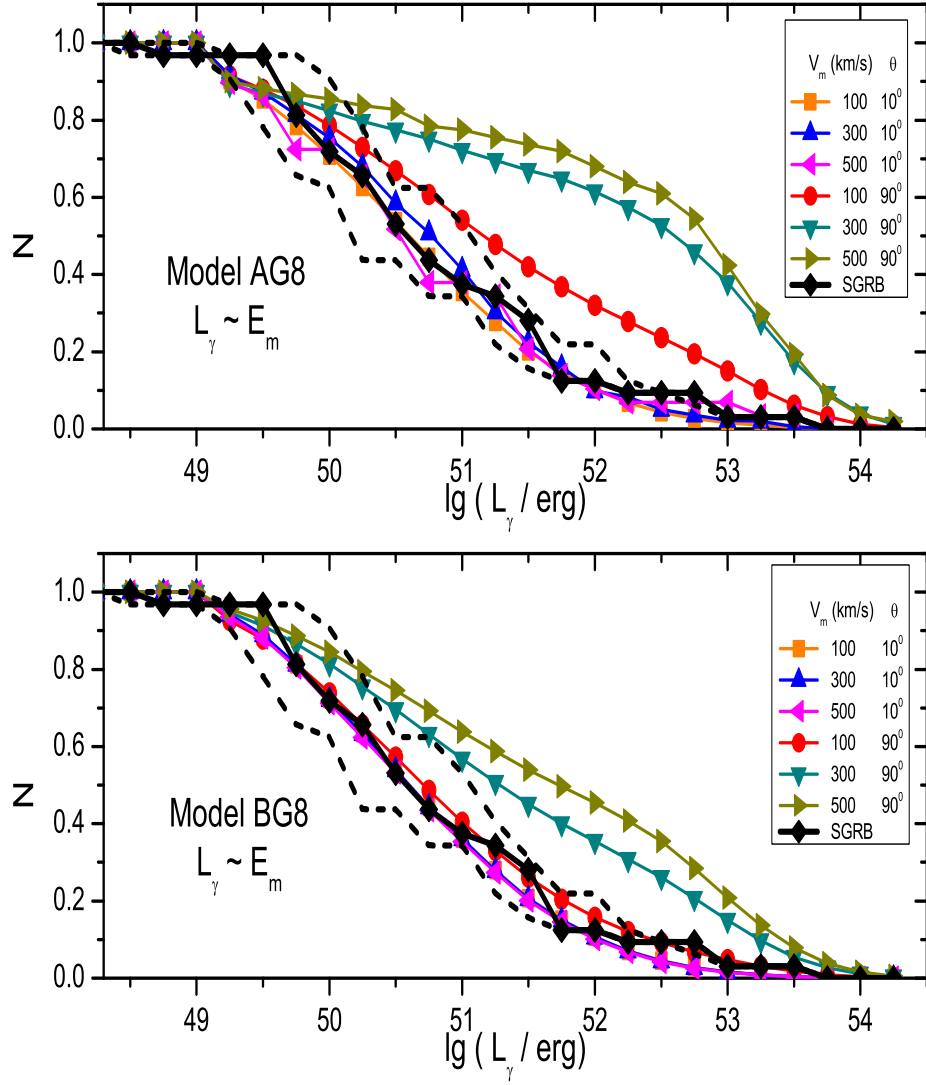


Figure 7. The comparison of the hypothesis  $L_\gamma \propto E_m$  for the luminosity of short gamma-ray bursts in models with exponential field decay AG8 (the upper panel) and BG8 (the bottom panel) for the initial log-normal distribution of the poloidal magnetic field component of NS.